Proper Orthogonal Decomposition Analysis of Asymmetric Sprays of Large Two-Stroke Marine Diesel Engines

Imre G. Nagy[1,2*], Christos Papadopoulos[1], Lambros Kaiktsis[1]
[1]*National Technical University of Athens, School of Naval Architecture and Marine Engineering, Division of Marine Engineering, Athens, Greece*
[2]*Winterthur Gas & Diesel Ltd., Winterthur, Switzerland*
**Corresponding Author*

***Abstract:-*Low-dimensional modeling has proven its applicability in internal combustion engine research for comparison of simulated and experimental data, moreover in identification of instantaneous and time-dependent flow structures. The paper presents results of Proper Orthogonal Decomposition (POD) analysis of asymmetric spray jets emanating from large two-stroke marine Diesel engine injectors. The spray primary breakup is simulated by means of (three-dimensional) Large Eddy Simulation (LES) and characterized by a non-mean subtracting POD analysis. First, proper tests are performed to verify the independence of results on the number of snapshots and shedding cycles. The results of the present POD analysis demonstrate that the spray dynamics, focusing on the concentration and the velocity field, can be represented by a few dominant modes. In particular, for the concentration field, POD mode 1 contains approximately 80% of the total energy, whereas, the second most energetic POD mode captures5% of the energy. The concentration field LES results were thus accurately reconstructed in terms of only the first four dominant modes. The time coefficients of POD modes are characterized by means of spectral analysis. The present computational study demonstrates the role of Kelvin-Helmholtz instabilities of the spray shear layer in disintegrating the spray liquid core.**

***Keywords:-* Proper Orthogonal Decomposition, CFD, LES, Spray Breakup, Eccentric Nozzle, Coherent Structures, Large Marine Diesel Engines, Fuel Injector**

I. INTRODUCTION

Emission regulations and the requirement for a more efficient operation are the main driving forces in marine Diesel engine development; reduction of pollutant emissions and specific fuel oil consumption are thus the corresponding main goals. Research on reducing emissions in modern Diesel engines mainly focuses on nitric oxides (NOx) and soot reduction. Production of NOx is mainly associated with high local values of temperature and oxygen concentration. On the other hand, soot production is the outcome of locally rich combustion. To optimize combustion in modern Diesel engines, fuel spray atomization and the associated enhancement of fuel-air mixing is thus a critical factor, and its positive effect is supported by increased fuel injection pressure.

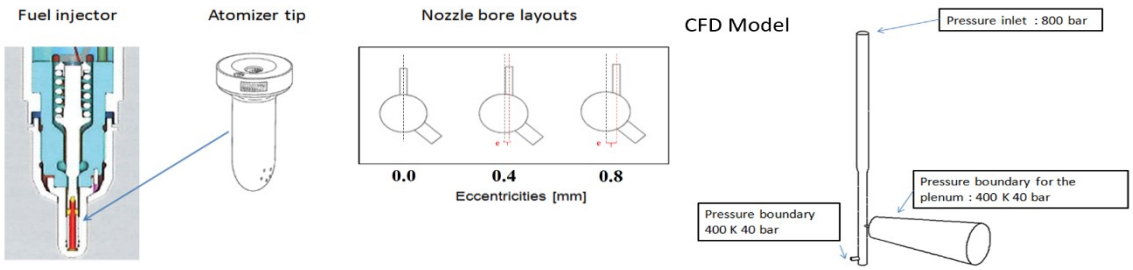

Figure 1. Conventional atomizer geometry with typical orifice distribution in two-stroke marine Diesel engines (left side), eccentric nozzle bore arrangements (middle) and the CFD model of the atomizer geometry with applied boundary conditions (right). [[4]]

In large two-stroke marine Diesel engines the injection system layout is peripheral, from two or more injectors, each with an appropriate number of orifices with different nozzle bore diameters. A number of five orifices is representative for such injectors, each of a size and injection direction aiming at an optimal dispersion of fuel into the combustion chamber [[1]-[2]].

Several studies have investigated the symmetric spray formation and the overall effects of fuel injection process on combustion. However, in marine Diesel engines, it is typical

for orifices to be arranged eccentrically with respect to the central bore axis of the injector (see Figure 1, middle), thus creating a highly asymmetric spray structure. The generated vorticity and fundamental instability inside the cylinder exhibits highly transient complex characteristics, which are expected to affect the turbulent fuel-air mixing. In particular, turbulent velocity fluctuations substantially affect mixing and the transfer of momentum, energy and species.

In our previous work reported in [[4]], CFD simulations have shown that the eccentric nozzle geometry results in a highly asymmetric spray structure. It has been realized that the layout of nozzles not only gives an increasing deflection at higher orifice eccentricity (with respect to the atomizer axis), but the spray also deviates from its own symmetry line, in an upward direction. In another study, we have investigated the primary breakup and structure of diesel spray generated by atomizers with different eccentricities [[5]]. In [[5]], the coherent structures in the vicinity of the atomizer orifice have been identified by applying the 'Q-criterion' vortex tracking technique of Hunt *et al*. [[6]].A similar approach has been used in [[7]] and [[8]], for analyzing flow dynamics of a transverse jet in crossflow, and in [[9]] for visualizing is surfaces of vorticity magnitude. In the context of diesel spray applications, these literature studies suggest that coherent structures substantially affect the distribution of fuel within the flow field.

The POD method has been extensively used over the last two decades in several applications of thermofluids, ranging from incompressible flows to engine flows and sprays[[10]-[19]]. Qin*et al*.[[20]] has investigated the spatial and temporal evolution of in-cylinder spray characteristics by applying POD on Mie-scattered spray images. Here, it has been found that the mean field contains more than 90% of the total intensity. In [[21],[22]],POD technique has been applied on the scalar field (combustion images), suggesting that POD contributes useful information for combustion variation.POD analysis has been used to the characterization of large and small structures of fuel spray data [[23]], while in [[24]] the method of snapshots has been implemented to the POD analysis of a subsonic jet computed by LES. Chen H. and Xu M. [[25]] have conducted the POD analysis in order to distinguish spray structure variations from different engine conditions by using 50 snapshots to reach convergence.

In the present work, a 3-D non-mean subtracting POD approach is implemented, in the context of the method of snapshots, to the analysis of our simulation results of asymmetric diesel sprays. These results, reported in [[4]] and [[5]], are the outcome of a coupled Volume of Fluid (VOF) – LES approach, focusing on the primary spray breakup, and have demonstrated the significance of nozzle geometry on spray formation. Specifically, in the current study, POD analysis is applied to the velocity and scalar fields of a non-evaporating spray emanating from an eccentric atomizer, calculated by the VOF – LES approach. These findings are used to reveal the properties of coherent flow structures identified and distributes among the POD modes.

The paper is organized as follows: The POD methodology is first briefly presented, followed by the presentation of the problem geometry and numerical approach. Results are then presented and discussed, and the main conclusions are summarized.

II. POD ANALYSIS

POD is a powerful approach for analyzing large computational and experimental datasets describing the response of dynamical systems, with the aim of identifying low-order models that capture the dominant system dynamics. POD has been introduced in the field of fluid mechanics by Lumley [[26]]. It has gained significant popularity in the last three decades, for the analysis of simulation and experimental data. Using numerical or experimental data, the method identifies the basis functions (proper orthogonalmodes), which optimally capture the system energy. As a result, the system dynamics can be accurately reproduced by using an appropriate (finite) number of these functions and proper time-dependent coefficients; the latter are calculated by projecting the data onto the computed modes. By projecting the governing equations onto these modes, it is possible to obtain low-dimensional ordinary differential equation models for a system such as a fluid flow. To minimize the cost of calculating the spatial modes (eigen functions), Sirovich introduced the 'method of snapshots'[[27]], also adopted in the present study.

In the present work, the tangential, radial and axial fluctuating velocity components of the spray jet, (functions of space and time)are denoted by $\vec{\mathbf{v}}(\boldsymbol{x},t)$={u, v, w}.All velocity fluctuation vectors are arranged in the following matrix (U), with k being the number of points in space and m the number of snapshots (points in time). It is noted that POD analysis can be performed both for the fluctuating velocity vector and for each of the individual components.

$$\mathrm{U} = \left[\vec{\mathbf{v}}^1\vec{\mathbf{v}}^2 \ldots \vec{\mathbf{v}}^{\mathrm{k}}\right] = \begin{bmatrix} \begin{pmatrix} \mathrm{u}_1^1 & \mathrm{u}_1^2 & \mathrm{u}_1^3 & \cdots & \cdots & \mathrm{u}_1^{\mathrm{k}} \\ \vdots & \vdots & \vdots & \vdots & \vdots & \vdots \\ \mathrm{u}_{\mathrm{m}}^1 & \mathrm{u}_{\mathrm{m}}^2 & \mathrm{u}_{\mathrm{m}}^3 & \cdots & \cdots & \mathrm{u}_{\mathrm{m}}^{\mathrm{k}} \end{pmatrix} \\ \begin{pmatrix} \mathrm{v}_1^1 & \mathrm{v}_1^2 & \mathrm{v}_1^3 & \cdots & \cdots & \mathrm{v}_1^{\mathrm{k}} \\ \vdots & \vdots & \vdots & \vdots & \vdots & \vdots \\ \mathrm{v}_{\mathrm{m}}^1 & \mathrm{v}_{\mathrm{m}}^2 & \mathrm{v}_{\mathrm{m}}^3 & \cdots & \cdots & \mathrm{v}_{\mathrm{m}}^{\mathrm{k}} \end{pmatrix} \\ \begin{pmatrix} \mathrm{w}_1^1 & \mathrm{w}_1^2 & \mathrm{w}_1^3 & \cdots & \cdots & \mathrm{w}_1^{\mathrm{k}} \\ \vdots & \vdots & \vdots & \vdots & \vdots & \vdots \\ \mathrm{w}_{\mathrm{m}}^1 & \mathrm{w}_{\mathrm{m}}^2 & \mathrm{w}_{\mathrm{m}}^3 & \cdots & \cdots & \mathrm{w}_{\mathrm{m}}^{\mathrm{k}} \end{pmatrix} \end{bmatrix} \quad (1)$$

Next, the auto-covariance square matrix (3m x 3m) is created:

$$\Theta = U^T \cdot U \quad (2)$$

and the corresponding eigenvalue problem becomes

$$\Theta\varphi_i(\mathbf{x}) = \lambda_i\varphi_i(\mathbf{x}) \quad (3)$$

where $\varphi_i = \varphi_1 \ldots \varphi_m$ are the eigenvectors and λ_i are the eigenvalues. The magnitude of each eigenvalue is representative of the energy of the corresponding eigenmode (eigenvector); eigenvectors are commonly arranged in a decreasing order, i.e., from the most energetic to the least energetic modes ($\lambda_1 > \lambda_2 > \lambda_3 > .. > \lambda_m$) [[9]].

The eigenvectors of the aforementioned eigenvalue problem make up a basis for reconstructing the original fluctuation flow vector $\vec{\mathbf{v}}(\boldsymbol{x}, t)$:

$$\vec{\mathbf{v}}(\boldsymbol{x}, t) = \sum_{i=1}^{m} \alpha_i(t)\lambda_i\varphi_i(\mathbf{x}) \quad (4)$$

The low-order modes are usually associated with large-scale flow structures. If a flow contains such structures, these can be realized in the first few high-energy POD modes. Therefore, the fluctuating flow field can be sufficiently approximated by taking into account a proper number, p, of high-energy POD modes ($p < m$):

$$\vec{\mathbf{v}}(\boldsymbol{x}, t) = \sum_{i=1}^{p} \alpha_i(t)\lambda_i\varphi_i(\mathbf{x}) \quad (5)$$

According to Chatterjee [[28]], performing the POD analysis with or without subtracting the average does not affect the calculation, but only the interpretation of the results. It is commonly stated that the first mode of the POD analysis is equivalent to the mean of the ensemble. Siegel *et al*. (2007) has performed POD without subtracting the mean flow on a generic wake flow developing a von Karman vortex street behind a D shaped cylinder. Here, it is stated that the first POD mode will typically be the mean flow, which is followed by large scale fluctuating modes, in this particular case, representing the von Karman vortex street.H. Chen in [[30]] has aimed to reveal the extent of importance of subtracting or not subtracting the ensemble average prior to performing the POD analysis. In this particular investigation, measured in-cylinder engine flows by POD analysis using 200 velocity field snapshots proved that POD mode 1 was an excellent estimate with respect to the kinetic energy. It has been shown that the energy content of POD mode 1 was approximately equal to, but slightly larger than, that of the ensemble-averaged value. M. El-Adaway in [[31]],has applied POD on velocity vector field images taken by utilizing Stereo-PIV technique inside an engine cylinder. This study has concluded, similarly to [[30]], that the resulted in flow pattern of the ensemble average was identical to POD mode 1 without subtracting the mean prior performing the POD analysis. In terms of energy content, it was found that POD mode 1 had slightly higher than that of the ensemble average value. The analysis has led to the conclusion that the first POD mode was an excellent estimate of, but not completely identical to, the ensemble average. In [[30]], argumentations for not subtracting the mean before executing a POD analysis have been discussed. It has been demonstrated that by keeping the ensemble average coefficients of POD mode 1 can reveal the extent to which the mean flow is present and its cycle-to-cycle variability. Further information on POD methodology and, the interpretation and application of subtracting and non-subtracting POD can be found in [[30],[39]].

In the present study, a non-mean subtracting POD implemented in Star-cd v.28, is applied on the scalar-velocity field.

III. PROBLEM SETUP AND NUMERICAL APPROACH

As part of our earlier research[[4]], [[5]], a combined RANS - LES simulation has been performed for different large two-stroke marine Diesel engine atomizer geometries, including in-nozzle flow under non-evaporating conditions (40 bar, 400 K). The spatial domain of the CFD simulations has consisted of the atomizer tip needle, the nozzle bore, with a diameter of 0.75 mm and a length of 4-5 mm, and the plenum, with a length of 15 mm. The domain has extended up to the bypass hole, of a diameter which accounted for the total area of the other four nozzle orifices of the actual injector (see Figure 1, right side). The spray primary breakup has been computed based on the approach of coupled Volume of Fluid (VOF) - Large Eddy Simulation (LES).To assess on the spatial resolution requirements of the LES calculations, prior transient in-nozzle flow simulations have been carried out with RANS turbulence modeling. Each RANS calculation has been integrated in timeup to 0.015s (for a large two-stroke engine operating at 100 RPM, this time corresponds to 3.25° of engine crank angle), until reaching a converged steady state solution; the results have been then used as initial conditions for LES calculations of different grid densities. For the RANS simulations, structured grids have been generated with the commercial software ICEM CFD, containing approximately 1 million cells. These calculations have been carried out with the Volume of Fluid (VOF) method and the High-Reynolds-number k-ε turbulence model. Turbulence parameters have been initialized after testing several values for turbulence intensity and length scale. The solution method utilized a velocity-pressure coupling based on the implicit SIMPLE method. The three-time level implicit Euler central differencing scheme has been applied. The time step has been fixed to a value of 0.0001 s, corresponding to values of the Courant (CFL) number in the range of 1-2.5. Since LES requires extensive computational resources, the aforementioned RANS results have been taken to initialize the

flow field for VOF-LES calculations. The Germano and Lilly dynamic Smagorinsky subgrid-scale turbulence model has been utilized, where, in addition to the low pass filter (at the level of numerical grid), a second spatial filter (the test filter)has been applied. The model coefficient has been determined dynamically, thus changing in time and space to account for the local state of turbulence. The time step has been adjusted to keep the CFL number under 0.2. The same boundary conditions as those of the RANS computations introduced above have been implemented. The LES computational domain has contained approximately 14 million cells, while a grid sensitivity analysis has been carried out, showing the importance of grid resolution on the resolved flow field.

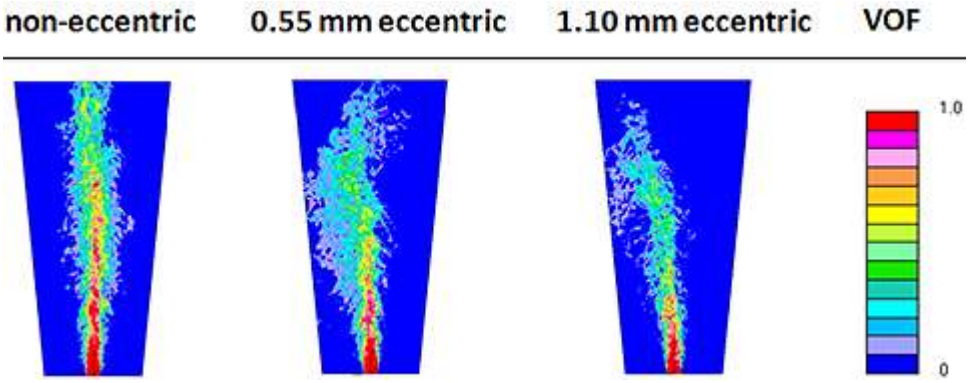

Figure 2. Distribution of liquid fuel concentration (void fraction) in the plenum for the three nozzle configurations (horizontal plane cut) after 0.2ms (equal with 0.12° engine crank angle) of LES time.

The computational time of the LES investigations has been correspondent to approximately 10 shedding periods of the emerging spray. The results have demonstrated that the eccentric nozzle geometry significantly affects the injected fuel, already within the nozzle bore. Surface disturbances have been initiated on the surface of the liquid right after entering the plenum. Here, the liquid surface has gone through a primary breakup process in the vicinity of the liquid core, mainly due to aerodynamic forces and turbulence induced atomization, resisted by the surface tension forces. Highly asymmetric spray behavior has been experienced for the different nozzle layouts. The resulting spray structures have been analyzed, and it has been illustrated that the eccentric arrangement of the nozzle results in a deflection normal to the main spray direction. The deflection has increased as a function of eccentricity. The results have shown that the spray has not been just deflected in the spanwise direction, but it also deviated from its symmetry line upwards, in the radial direction. Further information regarding the numerical setup, grid sensitivity analysis and the CFD modeling can be found in[[4]].

Nozzle eccentricity can substantially affect the resulting structure of spray flow, as illustrated in Figure 2, which shows the computed instantaneous fuel concentration (void fraction) in the horizontal plane crossing the plenum in the middle of the nozzle bore, for three values of nozzle eccentricity. These CFD results have been calculated using the VOF – LES approach with the Star-CD code [[40]]; the fuel thermophysical properties are those of n-Dodecane. In the present study, the nozzle characterized by an eccentricity of 0.55 mm has been chosen as the flow geometry of the POD analysis.

The LES results show that a statistical steady state is reached at a time of 0.2 ms (0.12° engine crank angle degree), at which the spray Reynolds number at the nozzle bore outlet is calculated. Here, a time-averaged velocity is considered, based on the velocity magnitude values in the last cell layer of the orifice.

$$\mathrm{Re_D} = \frac{\mathrm{U_D} \cdot \mathrm{D}}{\nu} = \frac{330 \cdot 0.00075}{1.8446 \cdot 10^{-6}} = 1.35 \cdot 10^5$$

Using the calculated Reynolds number of the turbulent flow, a typical Strouhal number (non-dimensional shedding frequency) can be defined for the spray jet, using a validated literature correlation. Typical values of Strouhal number for turbulent jet flows are in the range of$0.1 - 0.5$ [[41]-[46]].

$$\mathrm{St_D} = 0.198 \cdot \left(1 - \frac{19.7}{\mathrm{Re_D}}\right) \approx 0.198$$

This value is consistent with the results obtained by means of FFT analysis of the present LES results. The approximated vortex shedding frequency and period are calculated based on the spray Strouhal number.

$$\mathrm{f_D} = \frac{\mathrm{St_D} \cdot \mathrm{U_D}}{\mathrm{D}} = 88\ \mathrm{kHz}$$

$$T_D = \frac{1}{f_D} = 1.136 \cdot 10^{-5} \approx 1.14 \cdot 10^{-5}\ s$$

Siegel *et al*. (2015) has shown for time periodic flows modes identical to those calculated from snapshot based ensembles containing large number of shedding cycles can be obtained by using snapshot ensembles of small integer number of cycles, down to a minimum of one shedding cycle. Account on the validity of physical POD modes through transient flow situations, the POD analysis needs to be performed on a data set of relatively short length so that the POD modes represent the spatial flow features [[47]].

To characterize the turbulent spray jet flow, fourfull vortex shedding periods have been calculated for the spatial POD modes starting from the previously obtained RANS-LES results (approximately 1300 and 10 vortex shedding periods, respectively). A small constant time step of $\Delta t = 1e-09\ s$ has been chosen, maintaining the CFL number below 0.2.

$$T_{sim} = \sum_{4\ periods} 4 \cdot T_D = 4 \cdot 1.14 \cdot 10^{-5} = 4.6 \cdot 10^{-5}\ s$$

The completedata set utilized in the POD analysis consists of 150 snapshots, where the sampling interval has been correspondent to 0.67% of a shedding period.

IV. RESULTS AND DISCUSSION

Applying POD on the flow field provides an appropriate orthonormal basis to represent the flow. POD modes are sorted in an order of decreasing energy; thus, the first mode contains the maximum energy, and higher modes are characterized by a decreasing energy content. POD analysis reveals the dominant flow patterns, identifies large scale structures, and determines the number of modes necessary to reconstruct the flow fields, thus providing a reduced order representation of the flow. Large coherent structures are associated with the most energetic modes, while small structures are associated with the higher modes. In the present flow problem, the large structures are induced by Kelvin-Helmholtz instabilities in the shear layer of the spray, disintegrating further into ligaments and drops. To ensure the overall accuracy of POD analysis, different tests have been performed, varying (i) the number of snapshots for a constant time frame, and (ii) the number of shedding periods, for a given number of snapshots within one period. Results are presented next.

4.1Variation of number of snapshots

In varying the number of snapshots, the sampling time has been kept constant, equal to four shedding periods. Three tests have been performed, corresponding to a total of 50, 100 and 150 snapshots. Figure 3 shows the fractions of relative energy(multiplied by 100) captured by the first 15 POD modes for all three velocity components to determine the contribution of each mode to the original field. Different sample numbers of ensembles for four shedding cycles are considered.

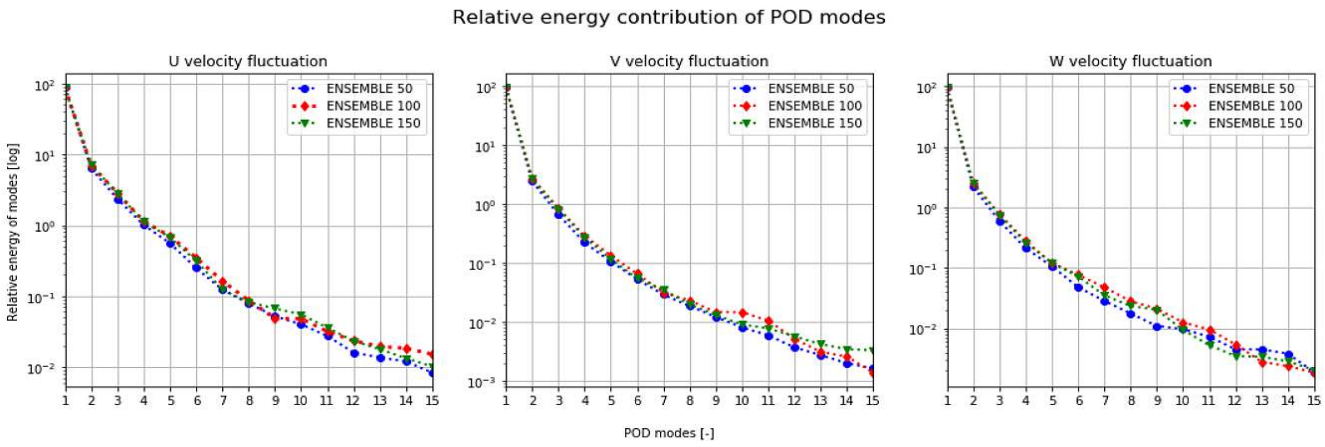

Figure 3. Mode relative energy, multiplied by 100, of the circumferential (U), the radial (V) and the axial (W) velocity component, for the 15 most energetic POD modes, computed for different numbers of snapshots. The sampling time is equal in all cases to four shedding cycles.

The corresponding cumulative energy content versus the number of modes is presented in Figure 4. The present results show a good agreement for all three numbers of snapshots, while the results for 100 and 150 snapshots nearly coincide. Similar observations have also been made regarding the concentration field (Figure 5). These findings are consistent with the observations in [[23]] for POD analysis of

experimental spray data. In summary, the analysis verifies that the number of snapshots used here is appropriate.

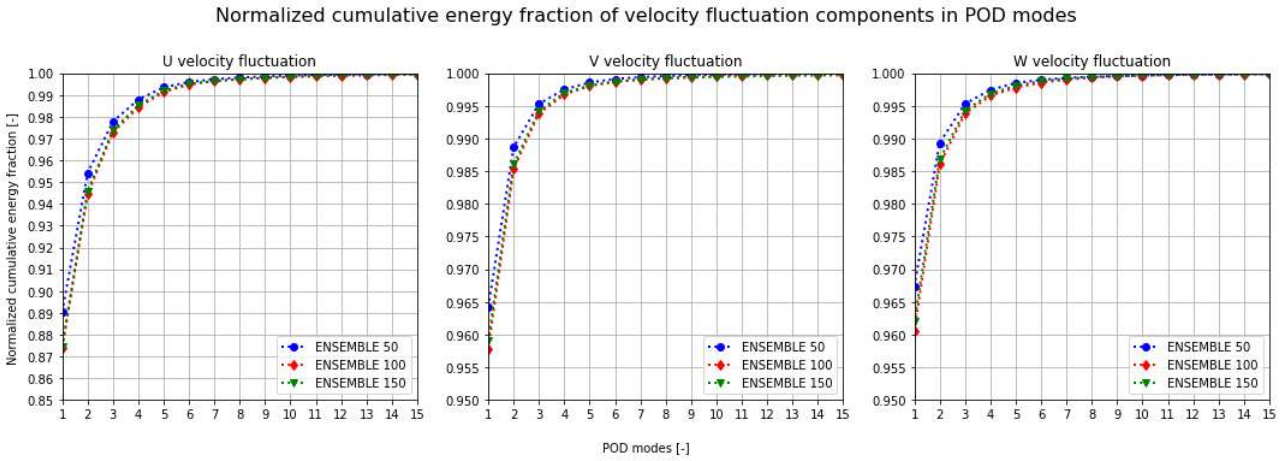

Figure 4. Cumulative energy versus number of modes, of the circumferential (U), the radial (V) and the axial (W) velocity component,up to the 15th most energetic POD mode, computed for different numbers of snapshots. The sampling time is equal in all cases to four shedding cycles.

Further, the present POD analysis of the velocity field shows that about 98% of the total energy is contained in the first four modes, and that practically all the energy is captured with very few modes (Figure 4.). Figure 5 presents the cumulative energy content of concentration field (void fraction). Here, POD mode 1 has approximately 80% of the energy, while the lower modes demonstrate relatively high energy contents (Mode 2 5%, Mode 3 2.5% and Mode 4 1.7%) compared to the velocity field modes. The results also reveal that POD mode 1 can be of the greatest contribution to the original flow field reconstruction. Furthermore, the presence of higher modes of the concentration field indicates the occurrence of small flow structures, what are still significant for turbulent mixing in the present spray jet problem.

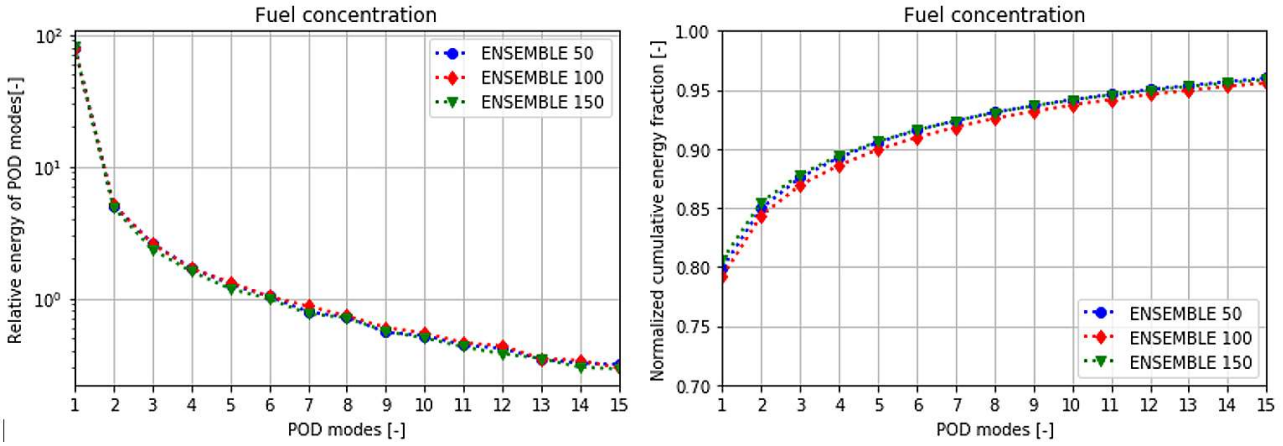

Figure 5. POD analysis of concentration (void fraction) field: mode relative energy, multiplied by 100 (left), and cumulative energy versus number of modes (right), up to the 15th most energetic mode, computed for different numbers of snapshots. The sampling time is equal in all cases to four shedding cycles.

4.2 Variation of spray vortex shedding periods

Next, the effect of varying the number of shedding periods on the results of POD analysis is checked, for a number of periods ranging from one to four. Using the outcome of the previous subsection (effects of varying the number of snapshots) the number of snapshots on the current variation is kept constant, equal to 50.

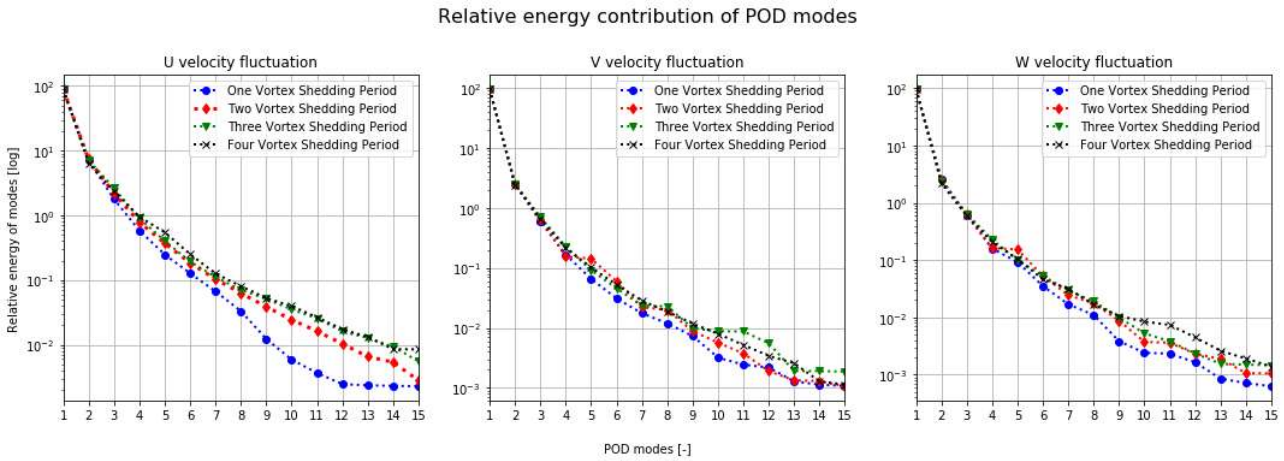

Figure 6. Mode relative energy, multiplied by 100, of the circumferential (U), the radial (V) and the axial (W) velocity component, for the 15 most energetic POD modes, computed for different numbers of shedding periods. A number of 50 snapshots is used in all cases.

Figure 6 presents the relative energies for the first 15 POD modes for all three velocity components, for different numbers of shedding periods. The corresponding cumulative energy versus the number of modes is presented in Figure 7. The current outcome shows that the discrepancies in energy content are rather small, and practically non-existing between the analyses for 3 and 4 periods. This also holds for the results regarding the liquid concentration (void fraction) field (Figure 8).

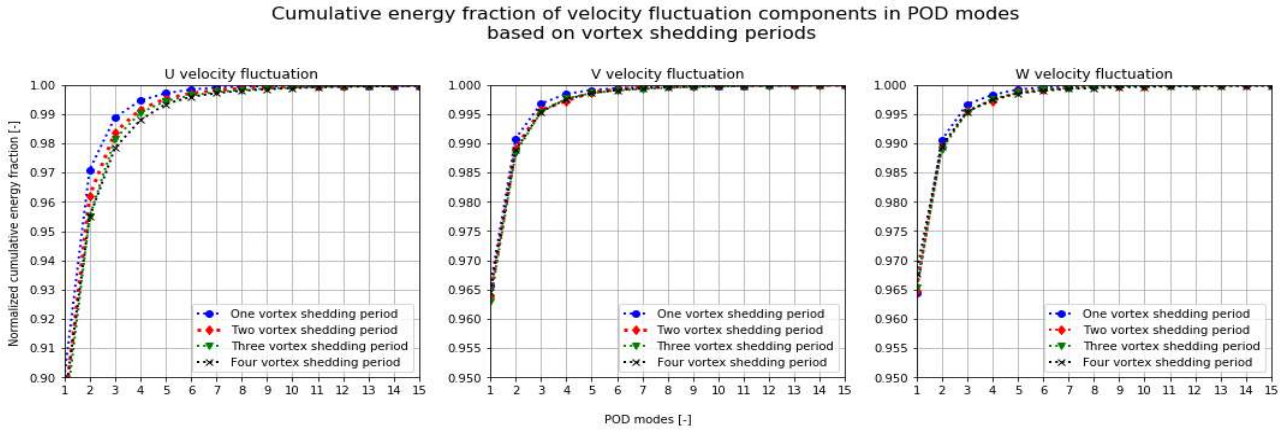

Figure 7. Cumulative energy versus number of modes, of the circumferential (U), the radial (V) and the axial (W) velocity component,up to the 15th most energetic POD mode, computed for different numbers of shedding periods. A number of 50 snapshots is used in all cases.

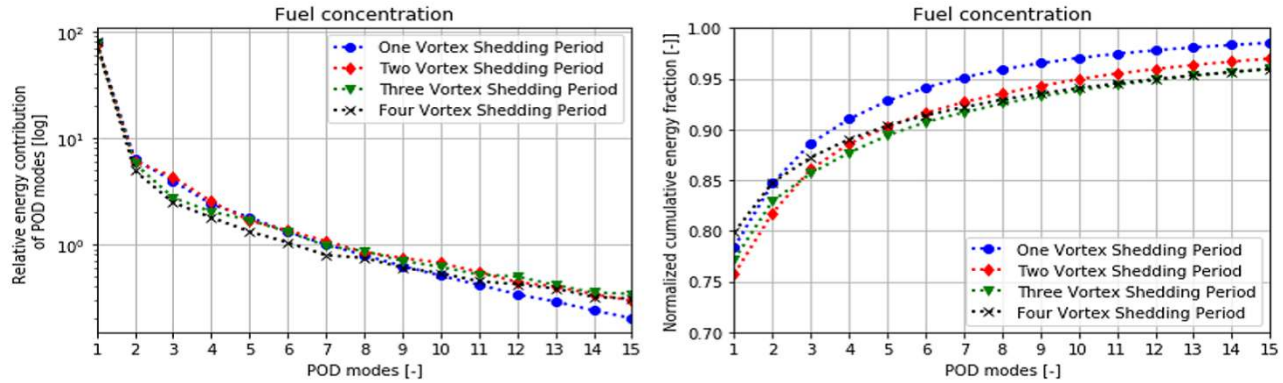

Figure 8.POD analysis of concentration (void fraction) field: mode relative energy, multiplied by 100 (left), and cumulative energy versus number of modes (right), up to the 15thmost energetic mode, computed for different numbers of shedding periods. A number of 50 snapshots is used in all cases.

Figure 9depicts a comparison of POD modes 2 and 3 of the three velocity components, for all four numbers of shedding periods used, verifying that the same mode structure is calculated for all values of flow sampling time considered. Focusing on spray primary breakup, disintegration of liquid blobs, ligaments and droplets from the liquid core at the air-liquid interface is expected. The analysis of POD modes can provide an insight of the mixing and explanation of spray fluctuation by extracting quantitative information on the characteristics of the spray atomization.

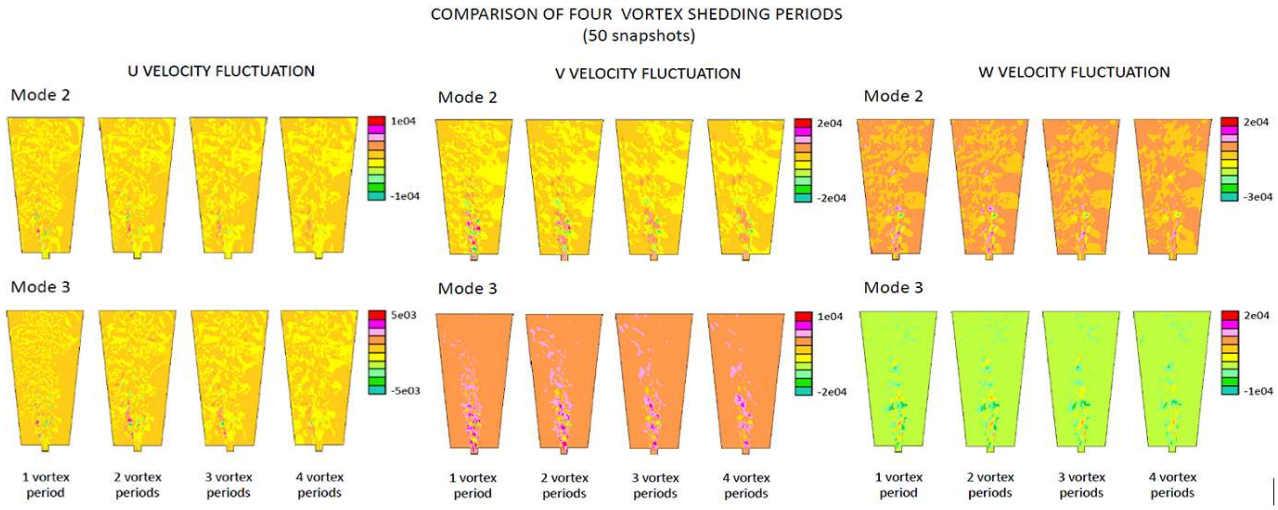

Figure 9. Small scale spatial flow structures of the 2nd and 3rd most energetic eigenmodes of the velocity component fields (horizontal plane cut).

In Figure 9, the velocity fluctuation fields are displayed by the contribution of POD mode 2 and 3, separately for each vortex shedding periods. The POD modes are characterized by positive (orange-red) and negative regions (yellow-green). The change of sign and color suggests a negative correlation in the simulated spray velocity fluctuations. Interpreting these changes for the velocity fluctuation, the change in colors means deviations from the average calculated for this specific data set [[48]]. The circumferential velocity component shows clearly the asymmetric spray behavior, where on the left side of the spray, more disintegrating flow structures are identified. These structures could be referred to vortices generated by the intense air entrainment. The second POD mode of the radial velocity field shows a clear periodic pattern; flow structures with higher magnitude can be found in the vicinity of the orifice. Both mode 2 and 3 clearly show the spray deflection in the horizontal plane, bending on the left side of the nozzle bore. Downstream the nozzle orifice, these flow structures continuously lose their energy. The axial velocity field, approximately up to 5mm downstream the orifice, suggests a fairly symmetric spray behavior. In the orifice near field the spray has a high momentum and a bulk spray structure represents the penetrating spray. Large-scale structures degenerating from the core are mainly distributed along the spray penetrating direction inside the mixing zone. It can be stated that significant difference among the analyzed vortex shedding periods cannot be found.

4.3 POD modes and flow reconstruction

Results of POD analysis are presented next for a sampling time of four shedding periods. According to Holmes et al [[33]], the suggested criteria for reconstructing a low order system by summing up just the most dominant modes are, at least 90% of the total energy should be included, and the mode with energy fraction larger than 1% should be considered. By utilizing the criteria, in this specific study, the first 6 modes are required for the reconstruction of the ensemble-averaged flow field. G. Charalampous *et al*. (2019) has described in his study the morphology of cluster formation and their evolution by analyzing spray primary breakup of a co-axial airblast atomizer. Following his findings, this section attempts to describe the spray primary breakup by examining the spatial distribution of the six most energetic modes of the fuel concentration (void fraction) field presented in Figure 10.

Mode 1, containing approximately 80% of the total energy, is characterized by the bulk spray structure, and should be thus associated with the intact spray core emerging from the orifice and large structures forming in the shear layer region. The redistribution of mass from the continuous liquid are the large-scale flow structures induced by the Kelvin-Helmholtz instability due to the interaction of the liquid jet with the surrounding air. The change in color highlights the negative relation between the intact liquid core and the detached liquid elements. Mode 2 and 3, with an energy content of 5% and 2.5%, should be associated with the ligaments and blobs forming out of the disintegrating large structures.

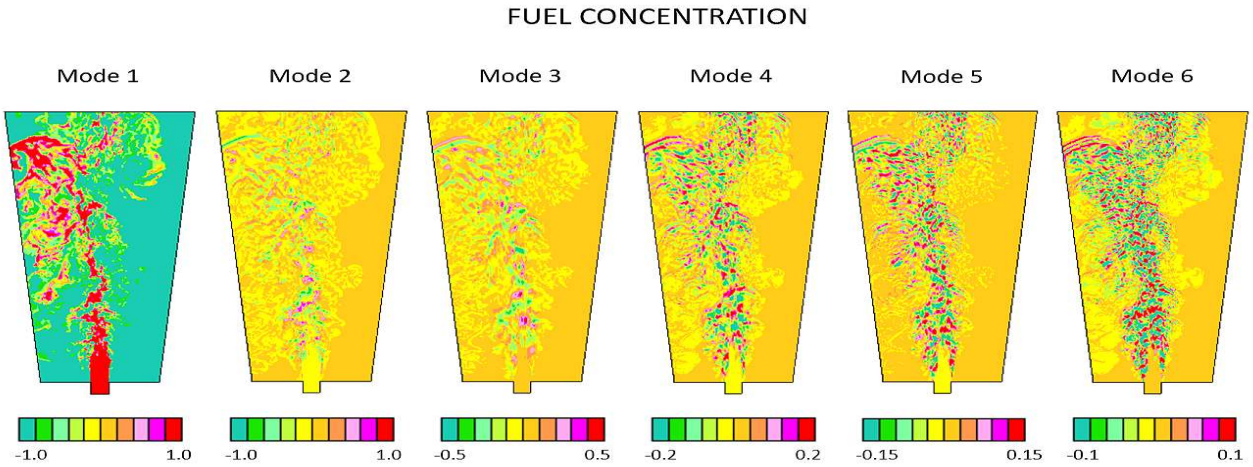

Figure 10. Spatial structure of the six most energetic eigenmodes of fuel concentration (void fraction) field (horizontal plane cut).

The atomization process presented by these modes is mild; droplet clusters formed out of the liquid core. Mode 3 shows longer nodes emerging from the nozzle than mode 2 and their presence of liquid suggests an inverse relationship.

Higher modes, characterized by finer scales, correspond to the smaller structures and droplets forming out of the disintegration of larger entities. In contrast, these modes represent the fine local details surrounding the edge of the spray and, a more chaotic behavior than the high-energy fraction containing lower modes. Mode 4-6 show the presence of more symmetric structures and capture well the asymmetric spray formation. These higher modes follow the droplet formation from their creation at the liquid jet surface and their transfer downstream. The spatial locations of the different modes do not coincide, since the air flow accelerates the disintegrated liquid particles. When a new breakup happens, the previously formed liquid structures are still adjacent (See POD mode 6). It is noted that the first four modes capture 90% of total energy, thus successfully depict the spray characteristics and in all cases taken, the mode structure reflects the spray asymmetry induced by the eccentric nozzle geoemtry.

A reconstruction of the instantaneous field, using the computed four spatial modes and corresponding time coefficients, is expected to provide a rather good representation of the instantaneous field. Indeed, the results presented in Figure 11 verify a very good comparison between the actual void fraction field, computed via LES, and the reconstructed field, at a time instant corresponding to the end of the sampling time. The ensemble average has similar, but not identical structure compared to POD mode 1,which suggests that the identified bulk spray structure can represent the spray characteristics and the higher modes have less significant roles. The reconstructed field is in a good agreement with the instantaneous field at each investigated cross section of the flow domain, proving that in this particular case, the first four most dominant modes are enough to represent the original flow field.

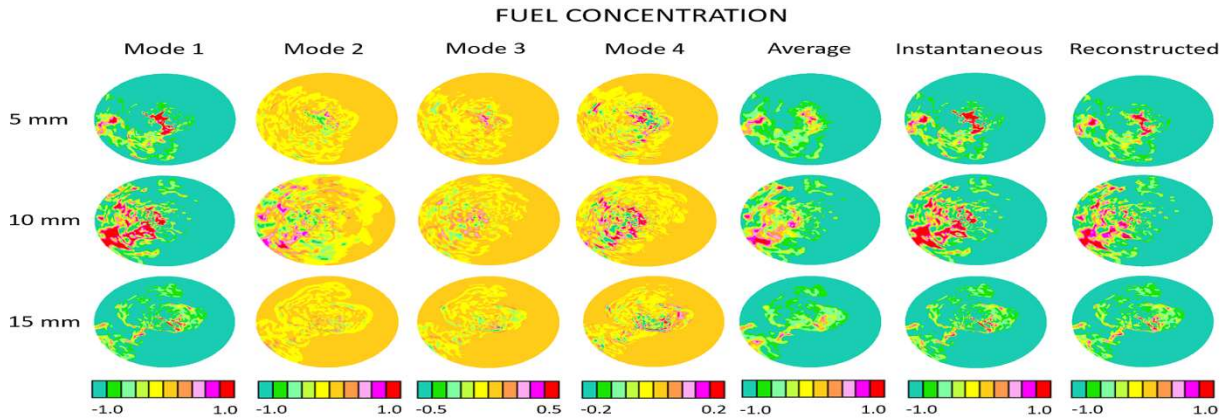

Figure 11.Spatial structure of fuel concentration (void fraction) at three representative cross-sections of the plenum: spatial structure of the four most energetic eigenmodes, computed time-averaged and instantaneous fields, and corresponding reconstructed field.

Similar outcome can be found in [[20]], where the temporal and spatial evolution of an in-cylinder fuel spray has been studied and in [[30],[31]], in case of POD applied in in-cylinder flow analysis. A possible even better comparison can evidently be attained by adding higher modes in reconstructing the instantaneous field.

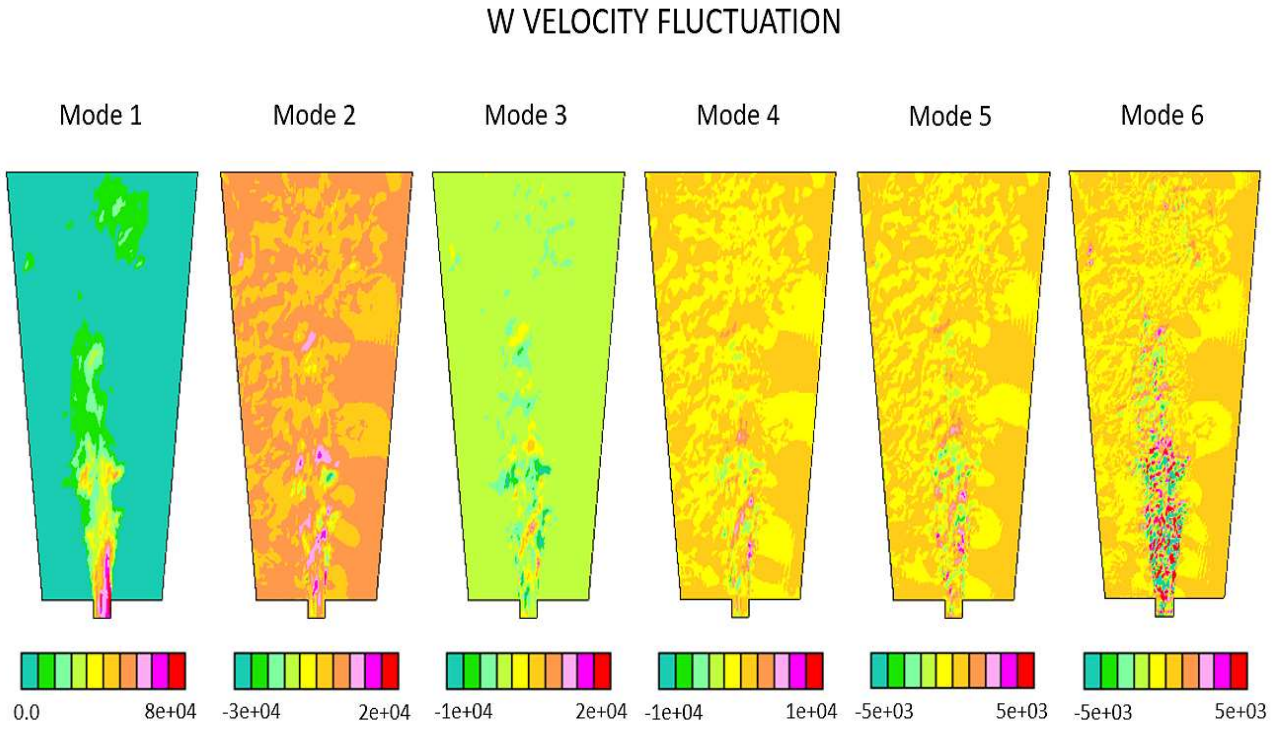

Figure 12. POD modes 1-6 of axial velocity fluctuation.

To characterize the spatial structure of velocity modes, the computed six most energetic modes of the W (axial) velocity component are presented in Figure 12. The spatial structure of the 1st mode is suggestive of axisymmetric type of shedding and showing a clear outline of the injected spray. High intensity of velocity fluctuations in the orifice near field can be realized by analyzing the 2nd and 3rd POD modes. Some of the higher modes are indicative of an azimuthal instability, while mode 6 is characteristic of the presence of small scales in a highly turbulent and chaotic flow.

4.4Temporal analysis of flow structures

The analysis of time coefficients may provide insight into the periodicity of features captured by the POD analysis and, the relation between different modes and the flow nature. Time coefficients are calculated by projecting the mean centered snapshot matrix onto the POD modes, and are represent the fraction of the POD mode that contributes to the snapshot. Negative or positive values of the time coefficient depicts the corresponding contribution of the analyzed POD mode to the particular snapshot.

Figure 13 presents phase-space plots of mode coefficients 2-5 versus the coefficint of mode 1 of the axial velocity component (analysis of 50 snaphsots). The presence of a symmetric distribution for mode 2 suggests symmetric shedding structures, while the skewed distributions for modes 3-5 suggest a correspondence with helical vortex structures in the shear layer regions.

The POD mode magnitude coefficients can be used for the analysis of spectral characteristics of the individual modes. The frequency content of POD modes can be identified by means of Fast Fourier Transformation (FFT) analysis (see also [[12]], [[49]-[52]]). In the current study, the Power Spectral Density (PSD) is used to execute the frequency spectral analysis. PSD describes how the power of a signal or time series is distributed over frequency. In this example, PSD represents simply the square of the real part of the frequency obtained from the FFT on the original signal. A similar approach has been utilized in the work of M. Khan *et al.* (2016) in order to identify and characterize coherent structures inside a gasoline injector nozzle.

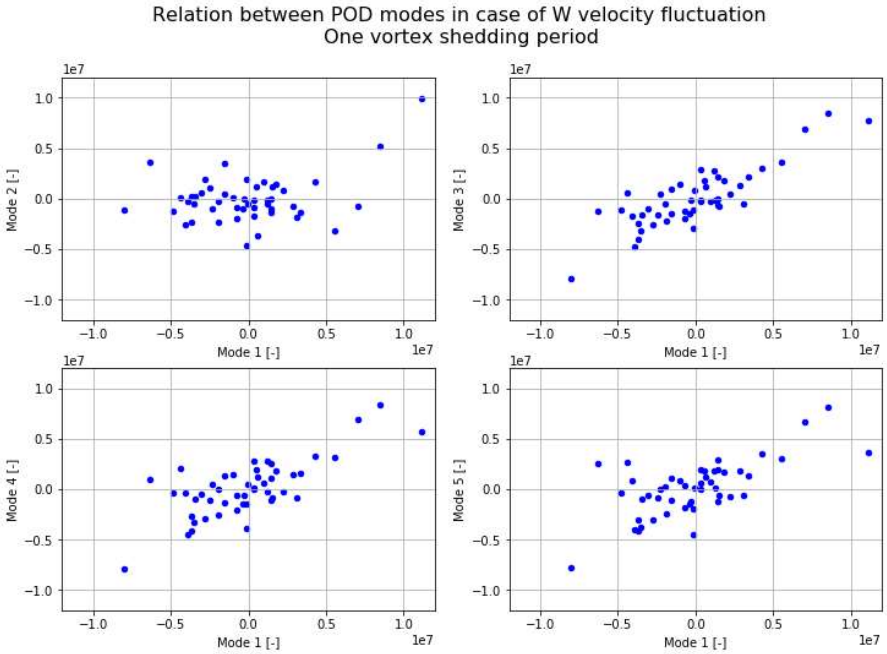

Figure 13. Streamwise velocity component: scatter plots of time coefficients of POD Modes 2-5 versus Mode 1coefficient.

Results are presented in Figure **14** for the axial velocity component mode coefficients. The modes demonstrate fairly identical temporal characteristics and a clear periodicity for each mode can be realized.

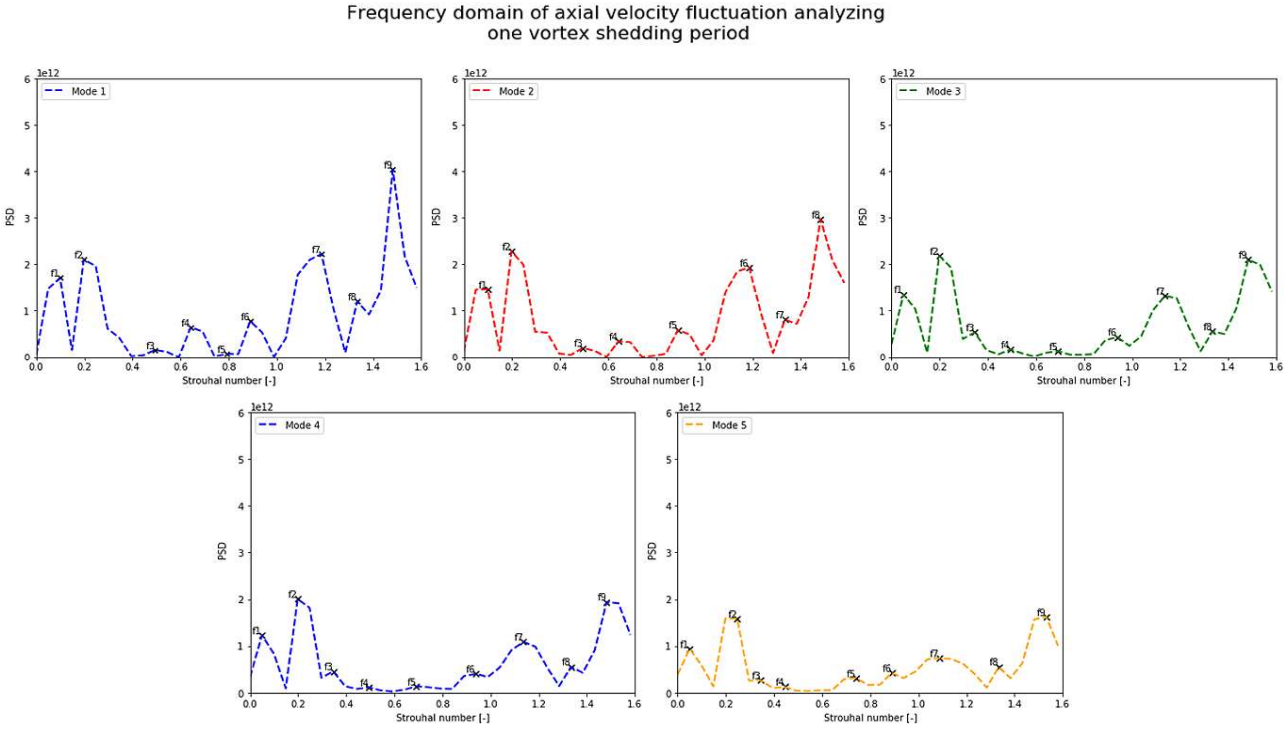

Figure 14. Calculated frequency spectra of time coefficients of axial velocity component POD modes 1-5

The outcome of the FFT analysis verifies the present of a non-dimensional frequency Strouhal number close to 0.2 and, in accordance with the value computed above by means of an established correlation, as well as the presence of a subharmonic and higher harmonics.

V. CONCLUSIONS

In the present study, an asymmetric diesel spray generated by an eccentric nozzle of a large two-stroke marine Diesel engine has been computed by means LES. A non-mean subtracting 3-D POD analysis has been implemented to characterize the calculated velocity and fuel concentration fields. POD can identify small-large characteristic scales; the calculated modes are correlated to disintegrating flow structures from the intact liquid core and can be interpreted as a liquid atomization process. Simulation results enlighten the role of Kelvin-Helmholtz instabilities in disintegrating the spray liquid core, generating ligaments and large droplets during primary breakup. The first POD mode qualitatively gives a very good estimate of the flow pattern of the ensemble average. The results demonstrate that the flow dynamics can be represented by a few dominant modes; thus, the flow field can be reconstructed by including the 4-5 most energetic modes. Analysis of time coefficients of the POD modes presents that they are characterized by dominant frequencies representative of turbulent axisymmetric jets.

ACKNOWLEDGMENTS

This research has received funding from the People Programme (Marie Curie Actions) of the European Union's Seventh Framework Programme FP7/2007-2013/ under REA grant agreement n° 607214– Experimental and Computational Tools for Combustion Optimization in Marine and Automotive Engines (ECCO-MATE). The authors would like to thank Mr. Alexandros Panagoulias of Siemens Industry Software GmbH, for his support and helpful discussions.

REFERENCES

[1] Weisser G. & Von Rotz B. & Schmid A. & Schulz R. & Herrmann K. Investigations into spray and combustion processes at conditions typical of large diesel engines making use of a spray combustion chamber specifically devised for this purpose. In:14. Tagung Der Arbeitporzess des Verbrennungsmotors, Graz, Austria, 24-25 September 2013.

[2] Schmid A. & Von Rotz B. & Schulz R. & Herrmann K. & Weisser G. &Bombach R. Influence of nozzle hole eccentricity on spray morphology. In: ILASS 2013, Chania, Greece, September 2013, DOI: 10.13140/2.1.2128.3209.

[3] Nagy I. G., Matrisciano A., Lehtiniemi H., Mauss F. Influence of nozzle eccentricity on spray structures in marine diesel sprays.In: 13th International Conference on Engines and Vehicles, Capri, Italy, September 2017, DOI:10.4271/2017-24-0031.

[4] Nagy I. G., Schmid A., Hensel S. &Dahnz C. Computational analysis of spray primary breakup in 2-stroke marine diesel engines with different nozzle layouts. In: 13th Triennial International Conference on Liquid Atomization and Spray Systems. (13), Tainan, Taiwan, 23-27 August 2015.

[5] Nagy I. G., Schmid A., Kaiktsis L. Characterization of asymmetric spray structures in large marine diesel engine sprays.,1stEcco-mate Conference, Lund, Sweden, 2016.

[6] Hunt J. C. R., Wray A. A. and Moin P. Eddies, streams, and convergence zones in turbulent zones.Proc. 1988 Summer Program, Stanford N.A.S.A. Centre for Turbulent Research, CTR-S88, November 1988.

[7] Zhang L. and Yang V. Flow dynamics and mixing of a transverse jet in crossflow – Part I: steady crossflow.*ASME Journal of Engineering for Gas Turbines and Power* 139(8), January 2017, DOI:10.1115/1.4035808.

[8] Zhang L. and Yang V. Flow dynamics and mixing of a transverse jet in crossflow – Part II: oscillating crossflow.*ASME Journal of Engineering for Gas Turbines and Power* 139(8), January 2017, DOI: 10.1115/1.4035809.

[9] Holmen V. *Methods for Vortex Identification*. Master Thesis, Numerical Methods and Fluid Mechanics, Lund University, November 2012.

[10] Meyer K. E., Cavar D. and Pedersen J.M. POD as tool for comparison of PIV and LES data. In:7thInternational Symposium on Particle Image Velocimetry., Faculty of Engineering, University La Sapienza, Roma, Italy, 11-14 September 2007.

[11] Kaiktsis L. and Monkewitz P. A. Global destabilization of flow over a backward-facing step. *Physics of Fluids*15(12):3647-3658,December 2003, DOI: 10.1063/1.1621003.

[12] Narayanan V., Lightfoot M. D. A., Schumaker S. A., Danczyk S. A. and Eilers B.Use of Proper Orthogonal Decomposition towards time-resolved image analysis of sprays. In: ILASS Americas, 23rd Annual Conference on Liquid Atomization and Spray Systems, Ventura, CA, May 2011.

[13] GamardS. and George W. K., Jung D., Woodward S. Application of a slice proper orthogonal decomposition to the far field of an axisymmetric turbulent jet.*Physics of Fluids*14(07), July 2002.

[14] Liu K. and Haworth D. C. Development and assessment of Proper Orthogonal Decomposition for analysis of turbulent flow in piston engines.SAE Technical papers, April 2011, DOI: 104271/2011-01-0830.

[15] Qin W., Xu M., Yin P., Hung David L. S. Analysis of the cycle-to-cycle variations of in-cylinder vortex structure and vorticity using phase-invariant Proper Orthogonal Decomposition., In: JSAE/SAE International Powertrains, Fuels and Lubricants Meeting, September 2015, DOI: 10.4271/2015-01-1904.

[16] Raposo J., Hentschel W., Merzkirch W.Analysis of the dynamical behavior of coherent structures in in-cylinder flows of internal combustion engines. In:In-cylinder flows of internal combustion engines, 10th International Symposium on Application of Laser Techniques to Fluid Mechanics, Lisbon, Portugal, 10-13 July 2000.

[17] Pastur L., Lusseyran F., Faure T., Podvin B. and Fraigneau Y. POD-based technique for 3D flow reconstruction using 2D data set., In:The 13th International Symposium on Flow Visualization 11(4):395-400, Nice, France, December 2008, DOI: 10.1007/BF03182208.

[18] Regert T., Rambaud P., Riethmuller M. R. Investigation of the link between physics and POD modes., In: Recent Developments in Non-Intrusive Measurement Technology for Military Application on Model-and Full-Scale Vehicles (pp. 4-1-4-12), Meeting ProceedingsRTO-MP-AVT-124 paper 4, Neuilly-sur-Seine, France:RTO., 2005.

[19] Kostas J., Soria J., Chong M. S. Particle Image Velocimetry measurement of a backward-facing step flow. *Experiments in Fluids* (2002), 33: 838-853, June 2002.

[20] Qin W., Hung D. L. S., Xu M. Investigation of the temporal evolution and spatial variation of in-cylinder engine fuel spray characteristics. In: *Energy Conversion and Management*, 98(2015), pp. 430-439, 2015.

[21] Bizon K., Continillo G., Leistner K. C., Mancaruseo E., Vaglieco B. M. POD-based anaylsis of cycle-to-cycle variations in an

optically accessible Diesel engine, *Proceedings of the Combustion Institute, 32(2009) pp. 2809-2816, 2009.*

[22] Bizon K., Continillo G., Mancaruseo E., Merola S. S. POD-based analysis of combustion images in optically accessible engines. In: *Combustion and Flame,* 157(2010) pp. 632-640, 2010.

[23] Tirunagari S., Hulkkonen T., Vourinen V., Kaario O., Larmi M. Proper Orthogonal Decomposition analysis of cross sectional fuel spray data.In: ICLASS 12th Triennial International Conference on Liquid Atomization and Spray Systems, Heidelberg, Germany, Sept. 2-6, 2012, DOI: 10.13140/RG.2.1.2395.4329.

[24] Tirunagari S., Vourinen V., Kaario O., Larmi M. Analysis of Proper Orthogonal Decomposition and Dynamic Mode Decomposition on LES of subsonic jets. *CSI Journal of Computing* 1(03), January 2012.

[25] Chen H., Xu M., Hung D. L. S., Yang J., Zhuang H. Development of a POD-based analysis approach for quantitative comparison of spray structure variations in a spar-ignition direct-injection engine. SAE International Conference, 2013, DOI:10.4271/2013-01-2545.

[26] Lumley J. L. The structure of inhomogeneous turbulent flows., In: Atmospheric Turbulence and Radio Wave Propagation, 166-178, 1967.

[27] Sirovich L. Turbulence and dynamics of coherent structures, Parts I-III.*Quarterly of Applied Mathematics* 45(03), pp. 561-571, October 1987, DOI: 10.1090/qam/910463.

[28] Chatterjee A. An introduction to the Proper Orthogonal Decomposition. *Current Science* 78(7), pp. 808-817, April 2000.

[29] Siegel S., Cohen K., Seidel J. and McLaughlin T. State estimation of transient flow fields using double Proper Orthogonal Decomposition (DPOD), Active Flow Control, NNFM 95, pp. 105-118, 2007.

[30] Chen H., Reuss D. L. and Sick V. On the use and interpretation of Proper Orthogonal Decomposition of in-cylinder engine flows. *Measurement Science and Technology* 23(2012), 085302, pp. 14, 2012.

[31] El-Adawy M., Heikal M. R., Aziz A. Rashid A., Adam I. K., Ismael M. A., Babiker M. E., Baharom M. B., Abidin F. and Abidin E. Z. Z. On the application of Proper Orthogonal Decomposition (POD) for in-cylinder flow analysis. In: Energies, 11(2018), 2261, DOI:10.3390/en11092261, 2018.

[32] Berkooz G., Holmes P. and Lumley J. L. The proper orthogonal decomposition in the analysis of turbulent flows.*Annual Review of Fluid Mechanics*25(01):539-575, pp. 539-575, 1993, DOI:10.1146/annurev.fl.25.010193.002543.

[33] Holmes P., Lumley J. L., Berkooz G., Rowely C. W.*Turbulence, Coherent Structures, Dynamical Systems and Symmetry*. 2nd editionCambridge University Press, 23 February 2012.

[34] Rowley C. W., Dawson S. T. M. Model reduction for flow analysis and control.*Annual Review of Fluid Mechanics*, Vol. 49, pp. 387-417, 2017.

[35] Kerschen G., Golinval J-C., Vakakis A. F. and Bergman L. A. The method of Proper Orthogonal Decomposition for dynamical characteristics and order reduction of mechanical systems: An Overview.*Non-linear Dynamics*41:147, pp. 147-169, 2005.

[36] George W. K. Insight into the Dynamics of Coherent Structures from a Proper Orthogonal Decomposition.Symposium on Near Wall Turbulence, Hemisphere, 1989.

[37] Taira K., Brunton S. L., Dawson S. T. M., Rowley C. W., Colonius T., McKeon B. J., Schmidt O. T., Gordeyev S., Theofilis V., Ukeiley L. S. Modal analysis of fluid flows: an overview.*AIAAAmerican Institute of Aeronautics and Astronautics*55(12), December 2017.

[38] Berkooz G., Holmes P., Lumley J. L. and Mattingly J. C. Low-dimensional models of coherent structures in turbulence.*Physics Reports*, Review Section of Physics Letters 287, N4:338-384, 1997.

[39] Meyer K. E., Pedersen J. M. and Ozcan O. A turbulent jet in crossflow analyzed with proper orthogonal decomposition.*Journal of Fluid Mechanics*583,pp. 199-227, DOI: 10.1017/S0022112007006143, 2007.

[40] Star-CD version 4.18, Methodology, LES models, Chapter 2, page 32, 2012.

[41] Khare P., Wang S., Yang V.Modeling of finite-size droplets and particles in multiphase flows.*Chinese Journal of Aeronautics*, 28(4), pp. 974-982, August 2015.

[42] Coltrin S., *The Influence of Nozzle Spacing and Diameter on the Acoustic Emissions of Closely Spaced Supersonic Jet Arrays*.Master Thesis, Brigham Young University, All theses and dissertations, Provo, February 2012.

[43] Webster D. R. and Longmire E. K. Vortex dynamics in jets from inclined nozzles. *Physics of Fluids* 9 (3), 1997.

[44] Duke D. J., Swantek A. B., Matusik K. E. and Powell C. F. X-ray radiography measurements and numerical simulations of cavitation in a metal nozzle.,In: ILASS Americas 28th Annual Conference on Liquid Atomization and Spray Systems, Dearborn, Michigan, May 2016.

[45] Ahmed M. H. and Barber T. J. POD convergence criterion for numerically solved periodic fluid flows.*WASE Transactions on Computer,* 5 1167-1172, January 2004.

[46] Arienti M., Corn M., Hagen G. S., Madabhushi R. K. and Soteriou M. C. Proper Orthogonal Decomposition applied to liquid jet dynamics.In: ILASS Americas, 21th Annual Conference on Liquid Atomization and Spray Systems, Orlando, Florida, 18-21 May2008.

[47] Siegel S., Cohen K., Seidel J. and McLaughlin T. Short time Proper Orthogonal Decomposition for state estimation of transient flow fields. 43rd AIAA Aerospace Sciences Meeting and Exhibit, Reno, Nevada, 10-13 January 2005.

[48] Charalampous G., Hadjiyiannis C. and Hardalupas Y. Proper Orthogonal Decomposition of primary breakup and spray in co-axial airblast atomizers, *Physics of Fluids* 31, 043304 (2019), DOI:10.1063/1.3263165, 2019.

[49] Khan M. M. and Sheikh N. A.Identification and characterization of coherent structures in gasoline injector nozzle flow using proper orthogonal decomposition.*Journal of Mechanical Science and Technology*, 30(8), pp. 3673-3680, 2016.

[50] Guadard E., Druault P., Marchiano R. and Van Herpe F. POD and Fourier analysis of a fluid-structure-acoustic interaction problem related to interior car noise.*Mechanics and Industry* 18(02), Art.no.:201, January 2017.

[51] Kypraiou M., Dowling A., Mastorakos E. and Karimi N. Proper Orthogonal Decomposition analysis of a turbulent swirling self-excited premixed flame, In: 53rd AIAA Aerospace Sciences Meeting, Kissimmee, Florida, United States of America, 5-9 January 2015.

[52] Charalampous G. and Hardalupas Y. Application of Proper Orthogonal Decomposition to the morphological analysis of confined co-axial jets of immiscible liquids with comparable densities. *Physics of Fluids* 26, 113301 (2014), DOI:10.1063/1.4900944, 2014.

[53] Charalampous G. and Hardalupas Y. Proper Orthogonal Decomposition analysis of photographic and optical connectivity time resolved images of an atomising liquid jet. In: ILASS-Europe 2011, 24th Annual Conference on Liquid Atomization and Spray Systems, Estoril, Portugal, September 2011.